

# Fabrication, testing and modeling of a new flexible armor inspired from natural fish scales and osteoderms

Ravi Kiran Chintapalli, Mohammad Mirkhalaf, Ahmad Khayer Dastjerdi and Francois Barthelat

Department of Mechanical Engineering, McGill University, 817 Sherbrooke Street West Montreal, QC, H3A 2K6, Canada

E-mail: [francois.barthelat@mcgill.ca](mailto:francois.barthelat@mcgill.ca)

Received 30 September 2013, revised 29 November 2013

Accepted for publication 14 January 2014

Published 11 March 2014

## Abstract

Crocodiles, armadillo, turtles, fish and many other animal species have evolved flexible armored skins in the form of hard scales or osteoderms, which can be described as hard plates of finite size embedded in softer tissues. The individual hard segments provide protection from predators, while the relative motion of these segments provides the flexibility required for efficient locomotion. In this work, we duplicated these broad concepts in a bio-inspired segmented armor. Hexagonal segments of well-defined size and shape were carved within a thin glass plate using laser engraving. The engraved plate was then placed on a soft substrate which simulated soft tissues, and then punctured with a sharp needle mounted on a miniature loading stage. The resistance of our segmented armor was significantly higher when smaller hexagons were used, and our bio-inspired segmented glass displayed an increase in puncture resistance of up to 70% compared to a continuous plate of glass of the same thickness. Detailed structural analyses aided by finite elements revealed that this extraordinary improvement is due to the reduced span of individual segments, which decreases flexural stresses and delays fracture. This effect can however only be achieved if the plates are at least 1000 stiffer than the underlying substrate, which is the case for natural armor systems. Our bio-inspired system also displayed many of the attributes of natural armors: flexible, robust with 'multi-hit' capabilities. This new segmented glass therefore suggests interesting bio-inspired strategies and mechanisms which could be systematically exploited in high-performance flexible armors. This study also provides new insights and a better understanding of the mechanics of natural armors such as scales and osteoderms.

Keywords: bio-inspiration, natural flexible dermal armor, segmented protective armor, fabrication and modeling

(Some figures may appear in colour only in the online journal)

## 1. Introduction

As a result of the 'evolutionary arms race' between predators and preys, animals such as mollusk shells, chitons, arthropods or turtles have developed protective systems with outstanding properties. The structure and mechanics of these natural armors have attracted an increasing amount of attention from research communities, in search of inspiration for new

protective systems and materials [1]. Nature has developed different strategies for armored protection against predators. While some protective systems are entirely rigid (mollusk shells) or with only a few degrees of freedom (chitons), a large number of animals also use segmented flexible armors in which the skin is covered or embedded with hard plates of finite size (typically at least an order of magnitude smaller than the size of the animal). Examples include the scaled skin

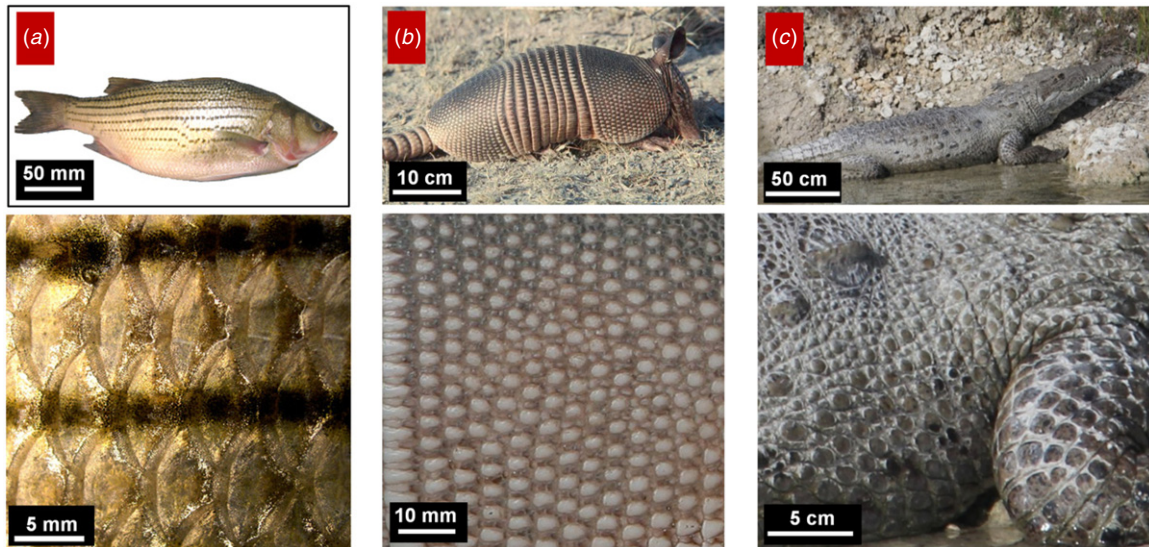


**Figure 1.** Examples of segmented natural armor: (a) fish (adapted from [4]), (b) armadillo [9] and (c) crocodile [10].

of fish, snakes or pangolin [2] (figure 1(a)), and osteoderms (bony plates embedded in the skin) in seahorses, armadillo or crocodiles, (figures 1(b) and (c)). Compared to rigid protective shells, segmented armors allow for much greater flexibility of movement, and they are therefore found in animal species with relatively fast locomotion. In this type of armor, individual hard plates provide resistance to puncture, and prevent the teeth of potential predators from penetrating the soft underlying tissues and vital organs. To fulfil this function, individual segments display highly efficient structures and mechanisms. For example, individual fish scales are multilayered plates which are 10 000 times stiffer than the underlying skin and tissues [3]. Scale are made of partially mineralized type I collagen fibers with a cross-ply structure [4]. Mineral content is significantly greater on the surface of the scale, which generates the hardness required to prevent penetration [2–6]. Meanwhile, the deeper layers are softer and can absorb more energy and provide a ‘membrane’ which contains the bony fragments in case they are fractured [4]. The osteoderm of armadillo is another interesting example of natural segmented armor, consisting of hexagonal and trapezoidal mineralized tiles with a uniform shape of approximately 5 mm in diameter and 1–2 mm thickness and covered by keratin [2, 7] (figure 1(b)). These hard tiles are connected with softer collagenous tissues, which hold the plates in place and limit excessive deflection of the skin [2, 7]. Crocodiles also have osteoderms that cover the entire body of the mammal, where individual segments are made of a porous bony core surrounded by dense bone. The skin is flexible yet highly resistant to puncture; it can resist arrows and even bullets [2].

There are three main strategies in flexible natural dermal armor [8, 10, 11]: (i) collagen fibers within the internal layer of the fish scales to provide flexibility (fish scales); (ii) flexible Sharpey’s fibers to connect tiles of osteoderms (armadillo); (iii) sutures to provide flexibility between hard plates (leather back turtle shells). In addition to flexibility of motion,

segmented protective systems are robust: even if one of the protective segments is destroyed or lost, the functionality of the rest of the skin is not compromised. In contrast, the fracture of rigid protective systems such as mollusk shells is usually fatal for the animal, which becomes at the mercy of predators. As a general rule, natural protective systems are also much stiffer and harder than the underlying soft tissues. For example, mollusk shells are about 6–8 orders of magnitude stiffer than the soft tissues they protect [11]. Fish scales are five orders of magnitude stiffer than the underlying skin and muscles. Armadillo tiles are 10–15 orders of magnitude stiffer than the underlying tissues mostly made of type I collagen fibers and osteons [3, 7, 12]. Combining materials with such large contrast of properties typically creates problems and precipitates failure due to mismatch of stresses. In this paper, we show how natural armors actually exploit this huge stiffness differential.

Natural armors have probably served as inspiration for personal armors throughout human history. For example, the *Lorica segmentata* was an armor made of several metallic plates used in ancient Rome. Traditional samurai armor contains small metallic plates sewn into thick fabrics, providing both protection and flexibility. More recently, segmented armor and fish-scale-like armor were proposed [13–17]. These armors consist of individual segments made of monolithic or composite material with predefined shape and size, held together by a flexible fabric or enveloped between two high tensile strength layers [16, 18, 19]. However, with the exception of a few recent studies [3, 20], the interplay of the hard protective plate on the soft substrate has received little attention. Here we systematically explore, for the first time, some key mechanics and design aspects for a flexible bio-inspired segmented armor consisting of transparent hexagonal glass plates on a soft rubber substrate.

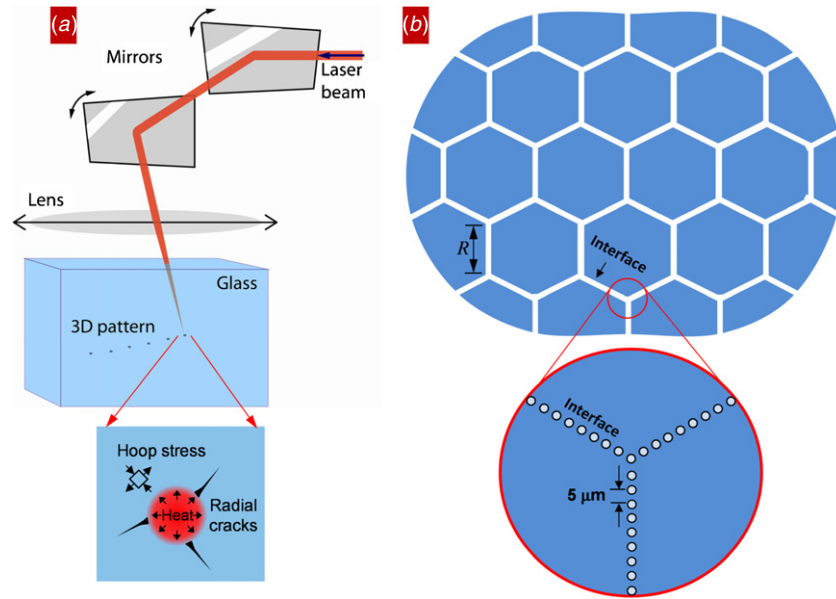


**Figure 2.** (a) Schematic of the laser engraving setup and (b) pattern geometry.

**2. Bio-inspired segmented armor: overview and fabrication**

The objective of this work was to duplicate a set of key attributes of natural segmented armors such as osteoderms and fish scales into a synthetic system. The key attributes we selected for this first biomimetic system consisted of hard protective plates of well-defined geometry, of finite size and arranged in a periodic fashion over a soft substrate several orders of magnitude less stiff than the plates. These attributes generate interesting capabilities such as resistance to puncture, flexural compliance, damage tolerance and ‘multi-hit’ capabilities. We chose a fabrication technique which enables the rapid and easy implementation of these attributes with a high level of geometrical control and repeatability. As a first model, we chose 150 μm thick hexagonal borosilicate glass plates as armor segments. The advantages of glass are its hardness and stiffness (we measured a modulus of 63 GPa for this particular glass using a three-point bending configuration). Glass is also transparent, a property we used here to generate hexagonal patterns by laser engraving. In this technique, a pulsed laser is focused at a predetermined point within the bulk of glass. While the power of the unfocused laser does not generate any structural change in glass, at the focal point the energy absorbed is sufficient to raise the temperature locally and generate microcracks from thermal stresses (figure 2(a)). Using this technique with a Vitromark ultraviolet laser at 100 mW power, we engraved hexagonal patterns within the glass slide, each line of the pattern consisting of a plane across the thickness of glass and made of hundreds of microcracks 5 μm apart (figure 2(b)). Following the concept of ‘stamp holes’, we adjusted the strength of the engraved lines by tuning the size and spacing of the defects. The resulting engraved lines were strong enough to prevent their fracture during handling, but weak enough for the hexagonal plates to detach during the puncture test. Hexagonal plates of different sizes were engraved, ranging from an edge length (*R*) of 0.25 to 6 mm

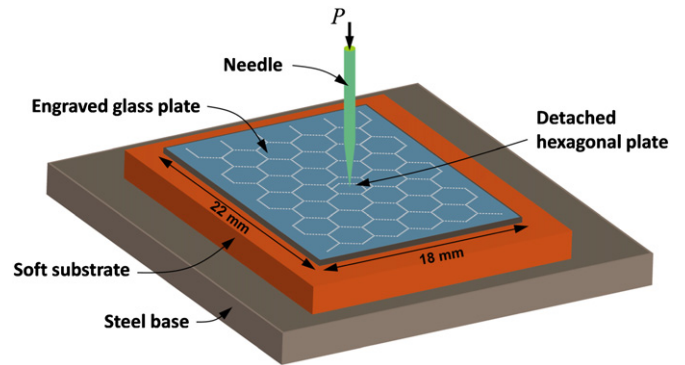


**Figure 3.** Test illustration of engraved glass under puncture tip- (a) engraved glass (b) shearing of hexagon.

(figure 2(b)). Once engraved, the plate was placed on a block of soft silicone rubber substrate which simulated soft tissues. We chose a relatively flexible rubber with a modulus of 1 MPa (measured by ball indentation), which is 63 000 times less stiff than the of glass plate. Our synthetic armor system therefore duplicated the main attributes of natural segmented protective system: hard and stiff individual plates of well-controlled shape and size, resting on a soft substrate several orders of magnitude softer than the plate.

**3. Puncture tests**

The puncture resistance of the glass layer was assessed with a setup we recently used to test natural fish scales [3, 4]. A sharp steel needle with a tip radius of 25 μm was attached to the crosshead of a miniature loading stage (Ernest F Fullam Inc., Latham, NY) equipped with a linear variable differential transformer and a 110 N load cell. The sample was positioned so that the steel needle would contact the plate in the central region of a hexagon. The steel needle was driven into the engraved glass at a rate of 0.005 mm s<sup>-1</sup> (figure 3) until the needle punctured the glass layer, a sudden event characterized

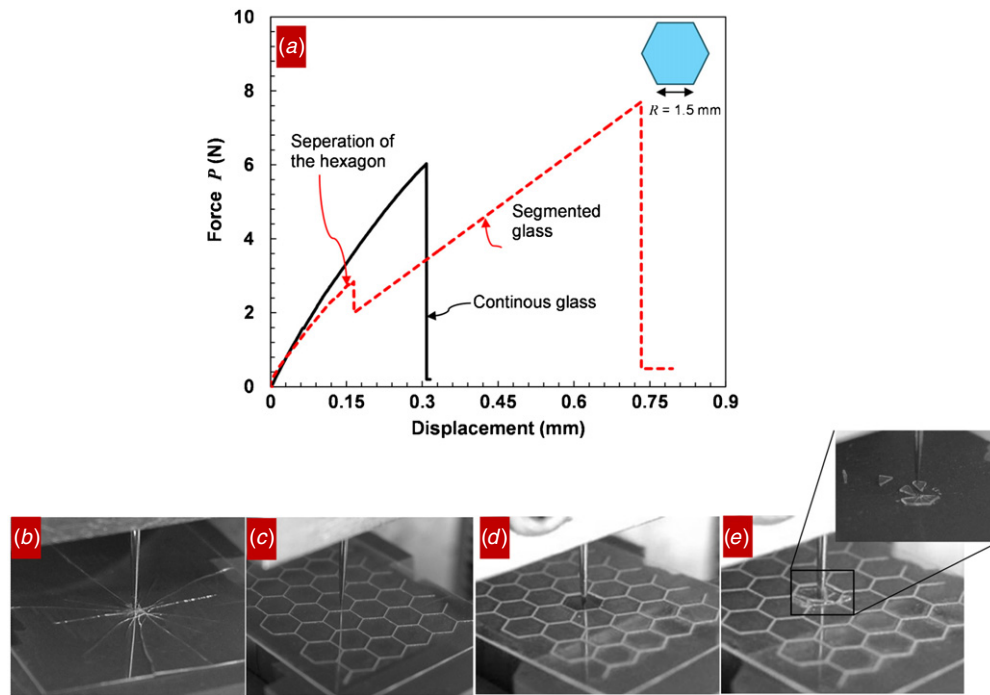


**Figure 4.** (a) Typical puncture force–displacement responses for a continuous glass plate and for segmented glass plate with  $R = 1.5$  mm; (b) failure mode for continuous glass plate; (c)–(e) failure sequence for segmented glass plate with  $R = 1.5$  mm.

by a sharp drop in force. As a reference, continuous glass (non-engraved) was also tested for puncture resistance under the similar loading conditions. The silicon rubber we used as a substrate had negligible resistance to sharp puncture.

Figure 4 shows typical results for the continuous glass plate, and for a segmented glass plate with hexagonal patterns ( $R = 2$  mm). The continuous glass slide shows a linear puncture force–displacement behavior up to a critical force of about  $P_{\text{crit}} = 6$  N, where the glass layer fractures abruptly (figure 4(a)). The glass plate shows several long radial cracks emanating from the tip of the needle, many of them reaching the edge of the plate (figure 4(b)). This type of crack behavior is a characteristic of a flexural failure of the glass plate [21, 22]. Under the point force imposed by the needle the glass plate bends, and flexural stresses increase. Tensile stresses are maximum just under the needle tip and at the lower face of the plate. In this region of the plate, the flexural stresses consist of radial and hoop tensile stresses, which are equal in magnitude. The hoop is responsible for generating the radial cracks observed in figure 4(b). Our system consisted of a thin plate on a soft substrate, so that failure from flexural stresses always prevailed over failure from contact stress [21, 22]. We confirmed this observation by interrupting a few puncture tests prior to the flexural fracture of the plate. No surface damage (indent, circumferential or conical cracks) was detected at and around the contact region, indicating that for all cases the fracture of the glass occurs from flexural stresses only.

The response to puncture of the segmented glass plate (hexagon size  $R = 2$  mm) was quite different from the continuous plate (figure 4). The initial response is identical, with a similar stiffness. At a force of about  $P = 2.5$  N a small drop in force is observed, corresponding to the fracture of the engraved contours of the punctured hexagon. After this

drop the hexagon is entirely detached from the rest of the plate, and is being pressed into the substrate by the needle. Further displacement requires increased force, but compared to the initial stage the stiffness is lower because it is ‘easier’ to push an individual hexagon into the substrate compared to the continuous plate. Eventually, the hexagon failed from flexural stress, developing multiple radial cracks. As opposed to the continuous plate, the cracks were all confined within the contour of the hexagonal plates. Interestingly, the critical force required to puncture the individual hexagon ( $P_{\text{crit}} = 7.5$  N) was higher than that for the continuous glass plate. The reason for this increase in puncture resistance is the result of the interplay between the soft substrate and reduced span as explained in the last section of the paper. In addition, the work to puncture, measured as the area under the force–displacement puncture curve, was seven times greater for the case of the segmented glass plate. The work required to fracture the glass plate is relatively small, so the increase of work is generated by the deformation of the softer substrate. For the continuous glass plate, the puncture force is distributed over a wide area at the plate–substrate interface, resulting in relatively small stresses and deformation in the substrate. In contrast, once the hexagon detaches from the segmented glass the puncture force is transmitted over a smaller area, with higher stresses transmitted to the substrate, resulting in larger deformations. In addition, the hexagon plate fracture at a higher force compared to continuous glass, further delaying fracture and leading to even more deformations in the substrate. For the case shown in figure 4, the displacement at failure is three times larger for the engraved glass compared to the intact glass. Higher force and displacement to failure lead to a much greater work to puncture, which is highly beneficial for impact situations. Figure 5 shows typical puncture force–displacement curves

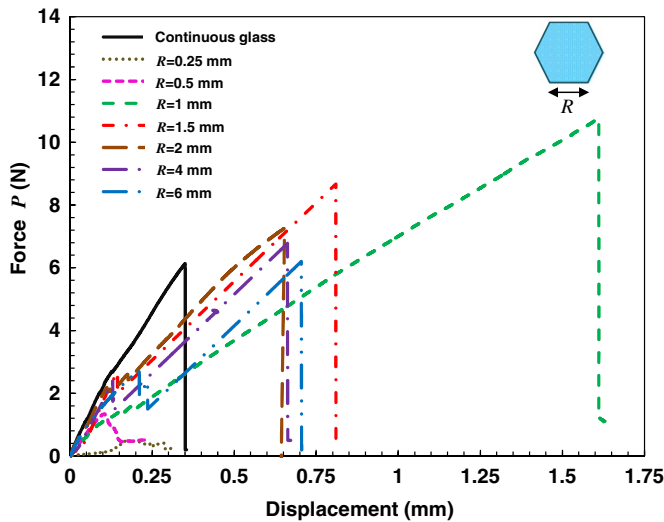


**Figure 5.** Typical force–displacement responses for continuous glass plate and for segmented glass plates.

for continuous glass and for the segmented glass with different hexagonal plate sizes.

As expected, the stiffness of the system after the hexagon was detached and was lower for the smaller hexagonal plate size. The critical puncture force is of particular interest, and it is shown in figure 6(a) as a function of hexagonal plate size

(we tested six samples for each size of hexagon). Most of the hexagonal plates failed by flexural cracking (figure 6(c)).

The results show that increasing the size of the hexagonal plates reduced the puncture resistance and work required until it reached the resistance of the continuous plate ( $P_{crit} = 6\text{ N}$ ,  $W_p = 1\text{ mJ}$ ), hexagonal plates of size 6 mm and larger essentially behaved like a continuous plate. On the other hand, as the hexagonal size was reduced the critical puncture force and work required were increased up to a maximum of  $P_{crit} = 9\text{ N}$ ,  $W_p = 7\text{ mJ}$  for  $R = 1\text{ mm}$ . This represents a 70% improvement over the puncture resistance of continuous glass. For hexagonal plates smaller than  $R = 1\text{ mm}$ , another failure mode prevailed: the individual hexagon tilted around the needle and largely lost contact with the substrate (figure 6(c)). This failure mode resulted in very low puncture force ( $P < 1\text{ N}$ ) and it is therefore highly detrimental to the performance of the armor. The failure mode transition from the hexagon fracture to hexagon tilting at a size of about  $R = 1\text{ mm}$  is probably governed by an interplay between the tablet size, substrate stiffness, adhesion between plates and substrate, and location of the puncture on the plate.

#### 4. Modeling flexural stresses

In this section, we investigated in more detail the mechanics behind the increase in performance experimentally observed for smaller hexagonal plates. Our starting hypotheses were that (i) flexural deformations and stresses dominate in stiff

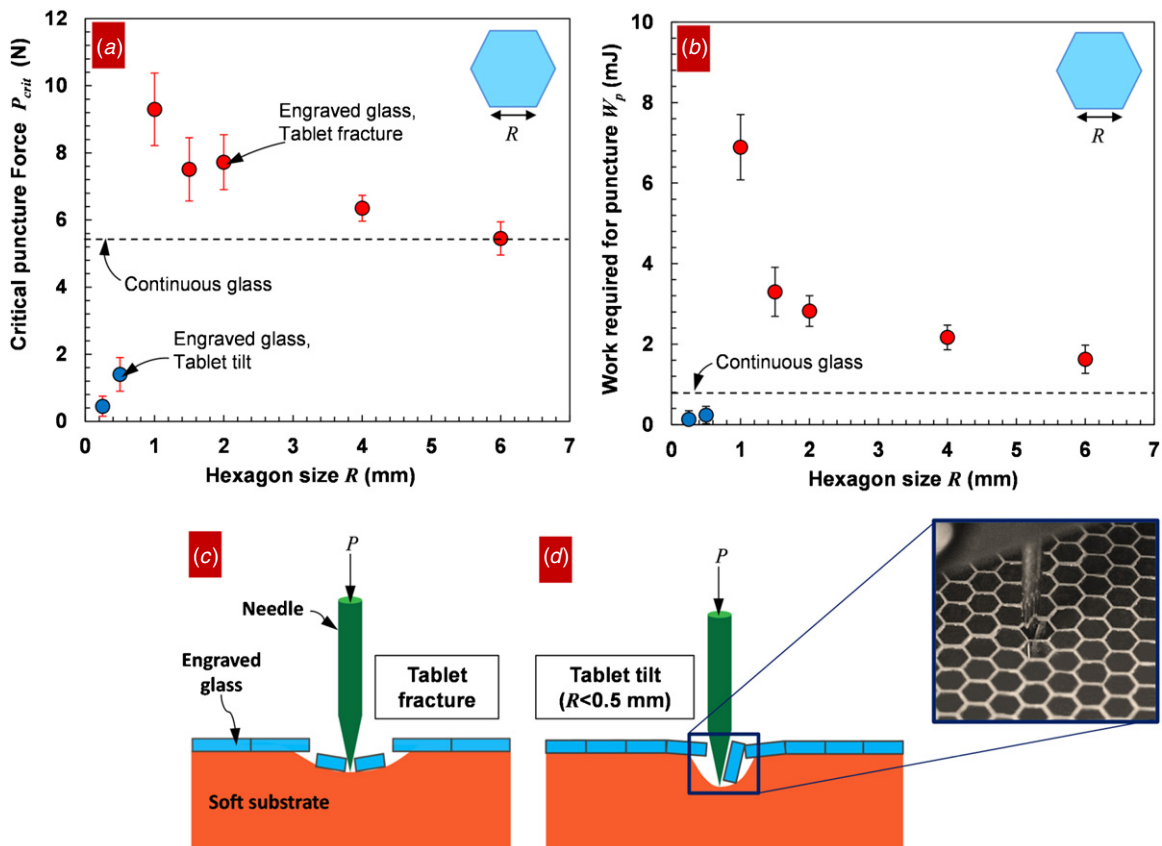


**Figure 6.** (a) Puncture resistance and (b) work required for puncture as a function of hexagonal plate size. Failure mode for (c) large hexagonal plates ( $R > 1\text{ mm}$ , red dots) and (d) small hexagonal plates ( $R < 1\text{ mm}$ , blue dots).

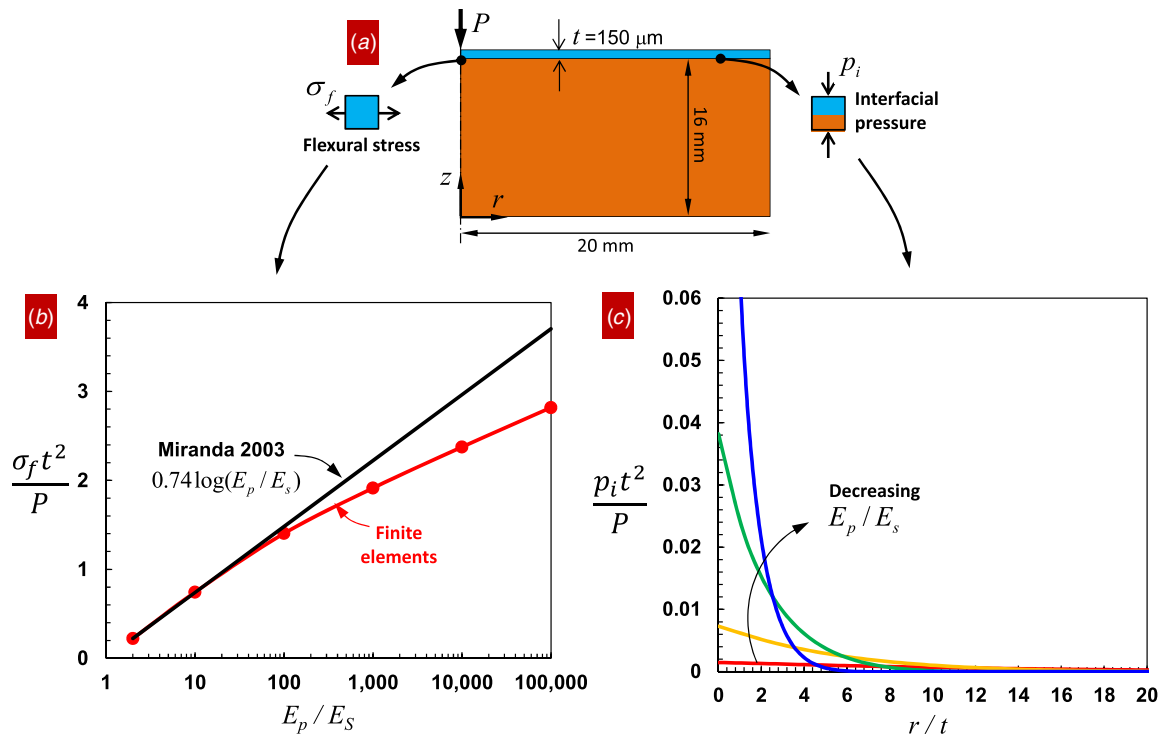


**Figure 7.** (a) Axisymmetric finite element model for a continuous plate on a soft substrate subjected to a point force  $P$ . (b) Maximum flexural stress (normalized with puncture force  $P$  and plate thickness  $t$ ) in the plate as a function of contrast of stiffness between the plate and substrate. (c) Distribution of interface pressure (normalized with puncture force  $P$  and plate thickness  $t$ ) for different contrasts.

plates on soft substrates and (ii) since smaller plates have a smaller flexural ‘span’ the flexural stresses are also smaller, and therefore smaller plates can undergo larger puncture forces before failing. To explore this scenario, the soft substrate and the stiff plate were modeled with finite elements [23]. We approximated the hexagonal plates as circular plates, in order to make use of the axial symmetry about the line of action of the force. An axisymmetric formulation was used for the elements, with the axis of symmetry of the model corresponding to the axis of the needle (figure 7(a)). Our first model consisted of a continuous plate (i.e. plate of infinite radius) resting on a soft substrate occupying a half-space. The system had a radius of 20 mm and the substrate was 16 mm thick, which we found was sufficiently large to model a continuous plate resting on a soft half-space (figure 7(a)). The plate (modulus  $E_p$ , Poisson’s ratio  $\nu_p$ ) has thickness  $t$  fixed at  $150 \mu\text{m}$  (thickness of the actual glass plate) and was assumed to be bonded on a softer substrate (modulus  $E_s$ , Poisson’s ratio  $\nu_s$ ). To investigate the effect of the contrast of properties between the plate and substrate, we fixed Poisson’s ratios at  $\nu_p = \nu_s = 0.2$  and we adjusted the contrast  $E_p / E_s$ . A mesh convergence study ensured that our results were not mesh sensitive. We also checked, using contact elements between the hard plate and the substrate, that the flexural stresses in the hard plate were not sensitive to the friction between the plate and substrate. The interface was therefore modeled as bonded to the substrate to save the computational time. The effect of the needle on the plate was modeled as a point force  $P$ , applied along the axis of symmetry (figure 7(a)). We did not try to capture the details of the contact stresses in the model, since the experiments showed

the absence of surface damage. We focused instead on the maximum flexural stress in the plate, which is located on the lower side of the plate underneath the application of the point force (figure 7(a)). The flexural stresses in the plate did not depend on whether the force was transmitted through a sharp contact or through a point force. A point force was therefore chosen to model the needle, in order to save the computational time. Figure 7(b) shows the maximum flexural stress in the plate as a function of stiffness contrast between the plate and substrate. As expected, softer substrates provide less support for the plate, which leads to higher flexural deformations and stresses. In the range  $1 < E_p / E_s < 100$ , we recovered the model from Miranda *et al* [24], but our results significantly deviated from this prediction for  $E_p / E_s > 100$ . This first model therefore shows that flexural stresses are prominent in stiff plates on soft substrates, and provide a baseline for the case of a continuous plate. It is also interesting to consider the distribution of pressure at the interface plate/substrate for various stiffness contrasts between the plate and substrate (figure 7(c)). For stiff substrates (small  $E_p / E_s$ ), the pressure is concentrated near the point force, while for soft substrate, the pressure is distributed over a much greater distance: the effects of the point force are ‘felt’ over a larger area in the case of softer substrates. This effect has direct implication on the mechanics of finite plates on the soft substrate, and on the performance of segmented armor.

Our second set of models consisted of a circular plate of variable radius  $R$  resting on a soft substrate (figure 8(a)). Again, we were interested in the maximum flexural stress in the plate, which occurs on the lower face of the plate and underneath

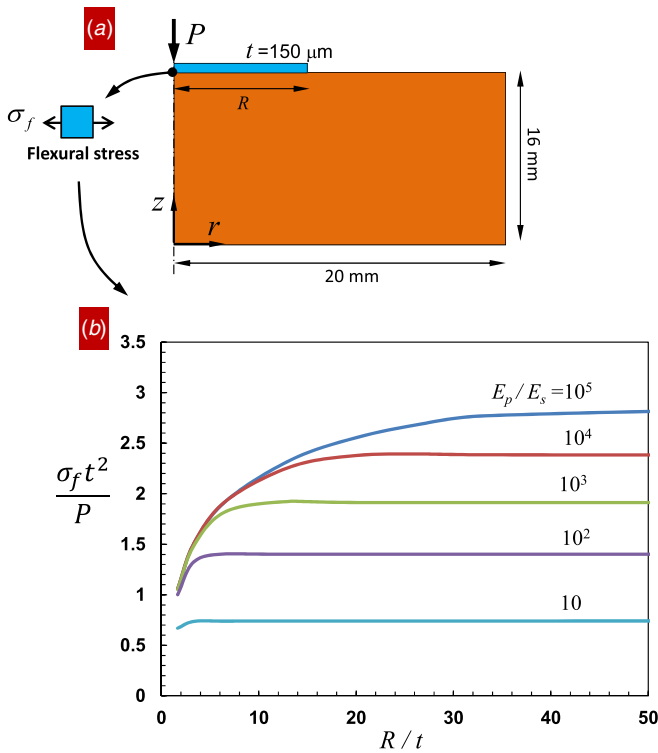


**Figure 8.** (a) Finite element model symmetry for a finite plate on a compliant substrate. (b) flexural stress (normalized with puncture force  $P$  and plate thickness  $t$ ) as a function of the contrast between plate and substrate.

the force. Figure 8(b) shows the normalized flexural stress as a function of normalized plate radius for four different contrasts between the modulus of the plate and the modulus of the substrate. The overall trend is similar to the behavior of the continuous plate. For a given plate thickness and applied force  $P$ , the flexural stresses are higher for softer substrates (i.e. higher  $E_p/E_s$ ). For all contrasts studied here, the results of the continuous plate are recovered for  $R/t > 40$ .

The results also show that in some cases the flexural stresses are significantly reduced for smaller plates. For low contrast, the flexural stresses are barely affected by the size of the plate. This can be explained in light of the results for the continuous plate (figure 7(c)): if the substrate is stiff only a small area around the point force is affected by the point force. As a result, reducing the size of the plate to a disc of finite radius has little effect on the stresses. In contrast, a soft substrate leads to a strong effect of  $R$  on the flexural plate. A continuous plate on a very soft substrate ‘feels’ the effects of a point force over a large area. Therefore, reducing the size of the plate has strong effects on the flexural stresses. Another way to interpret this result is by considering that reducing the size of the plate reduces its ‘flexural span’, in effect reducing bending moments and the flexural stresses. Finally, a last set of simulations was performed with the actual properties for the plate ( $E_p = 63$  GPa and  $\nu_p = 0.2$  for glass) and the substrate ( $E_s = 1.3$  MPa and  $\nu_s = 0.49$  for rubber). Note that modeling the rubber substrate with an incompressible Neo–Hookean model (shear modulus  $G = 0.65$  MPa) gave exactly the same

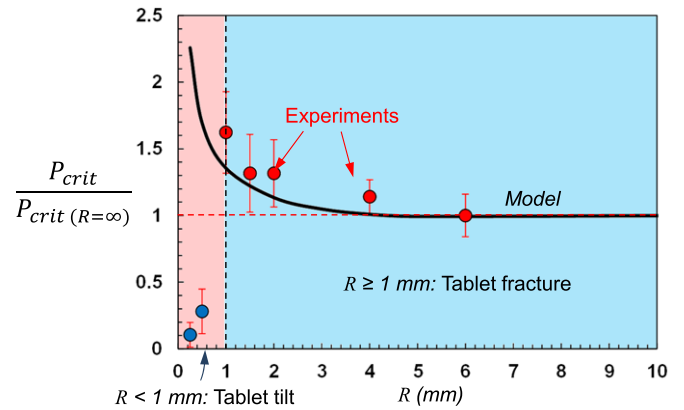


**Figure 9.** Normalized critical load as a function of plate radius  $R$  (size of hexagon). Note the failure mode transition from tablet fracture ( $R > 1$  mm) to tablet tilt ( $R < 1$  mm).

results. Here, it is useful to consider the critical force  $P_f$  at which the plate fails in flexion. To examine the effect of plate size, we then considered the ratio  $P_{crit}/P_{crit(R=+\infty)}$ , which is the critical force normalized by the critical force for a continuous plate ( $R = +\infty$ ) of the same thickness and made of the same material. This ratio is plotted as function of  $R$  in figure 9, together with the experimental data.

The model clearly shows that the force required to fracture the hexagonal segment is higher with decreasing segment size, and agrees well with the experiments. This result therefore suggests that the improved performance of the segmented plate is due to the reduced flexural span of the small hexagonal segments. The results of this model (figure 8) can also be used as a guideline for the design and dimensioning of stiff and hard protective plates on a soft substrate.

### 5. ‘Multi-hit’ capabilities, flexibility

Finally, we demonstrate the ‘multi-hit’ capabilities of the segmented plate. Figure 10(a) shows a segmented plate ( $R = 1.5$  mm) which was punctured four times at different locations, with an equally high performance for each puncture. As opposed to a continuous plate, puncturing one hexagon on the segmented plate does not compromise the performance of the rest of the plate, since damage is confined to the hexagon which was punctured. We also demonstrate how the segmented armor leads to high flexibility without compromising its puncture performance. A segmented glass plate was glued onto a 2 mm thick silicone rubber film with silicone glue. Applying a gentle bending to the composite film detached the hexagonal plates from one another. After this ‘breakdown’ operation, the silicone sheet could be bent by a large extent, demonstrating the flexibility of the segmented armor. Excessive bending led to the hexagonal plates detaching from the substrate, emphasizing the importance of a strong anchorage of the plates on the substrates for both natural and bio-inspired segmented armor.

### 6. Conclusions

Segmented armor systems are common in the animal world and found in many animal species across different families

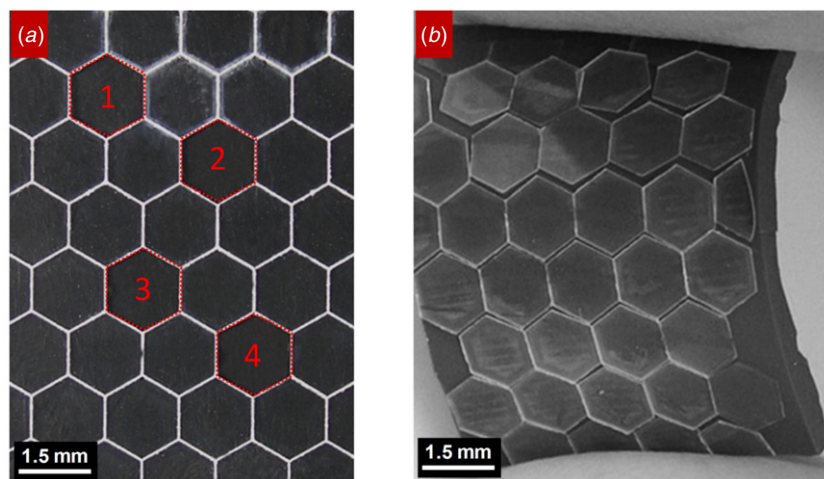


**Figure 10.** (a) ‘Multi-hit’ capability: puncturing one hexagon does not compromise the performance of the rest of the plate. Here, a segmented plate was punctured four times and (b) another plate was glued to the substrate using silicone glue, bending of the system detaches the hexagon, allowing for high flexibility.

and classes (fish, armadillo and crocodile). Segmented armors offer an elegant solution to solving the paradox of resisting puncture (requiring hard materials) while maintaining flexibility (requiring soft materials). Here, we have fabricated and tested a bio-inspired segmented armor made of hexagonal glass plates resting on a rubber substrate. Our main finding is that not only segmented plates provide flexibility to the much softer skin and underlying tissues, they also reduce flexural stresses and delay fracture. In the glass–rubber system we developed and studied here, the puncture resistance was increased by up to 70% using a segmented design (compared to the continuous plate). A detailed structural analysis of the system revealed that this remarkable increase in performance is due to the reduced span of the hexagonal plates in the segmented design. This effect can however only be achieved for high contrast in properties between the plates and substrate: the plates must be at least 1000 times stiffer than the substrate. The effect is also limited by the stability of individual plates: when the plates become too small they tend to tilt, a highly detrimental failure mode for the protective layer. The effect of the adhesion between the plate and substrate probably play a critical role here, which we are currently exploring. The remarkable performance of natural and bio-inspired segmented armor relies on the interplay between the plate size and contrast of stiffness between the plates and substrate. Our findings and models can be used to guide the design of bio-inspired segmented protective layers with application in protective coatings, personal armor or flexible electronics. They also provide new insights into the mechanics of natural scales and osteoderms.

### Acknowledgments

This research was supported by a Discovery Accelerator Supplement from the Natural Sciences and Engineering Research Council of Canada (NSERC). The three-dimensional laser engraver was purchased with a Research Tools and Instrumentation grant from NSERC. The mechanical testing facility was acquired through a grant from the Canada Foundation for Innovation (Leader Opportunity Fund).

### References

- [1] Bar-Cohen Y 2006 Biomimetics—using nature to inspire human innovation *Bioinspir. Biomim.* **1** P1–P12
- [2] Chen P-Y, McKittrick J and Meyers M A 2012 Biological materials: functional adaptations and bioinspired designs *Prog. Mater. Sci.* **57** 1492–704
- [3] Zhu D, Szewciw L, Vernerey F and Barthelat F 2013 Puncture resistance of the scaled skin from striped bass: collective mechanisms and inspiration for new flexible armor designs *J. Mech. Behav. Biomed. Mater.* **24** 30–40
- [4] Zhu D, Ortega C F, Motamedi R, Szewciw L, Vernerey F and Barthelat F 2012 Structure and mechanical performance of a ‘modern’ fish scale *Adv. Eng. Mater.* **14** B185–94
- [5] Bruet B J F, Song J, Boyce M C and Ortiz C 2008 Materials design principles of ancient fish armour *Nature Mater.* **7** 748–56
- [6] Song J, Ortiz C and Boyce M C 2011 Threat-protection mechanics of an armored fish *J. Mech. Behav. Biomed. Mater.* **4** 699–712
- [7] Chen I H, Kiang J H, Correa V, Lopez M I, Chen P-Y, McKittrick J and Meyers M A 2011 Armadillo armor: mechanical testing and micro-structural evaluation *J. Mech. Behav. Biomed. Mater.* **4** 713–22
- [8] Yang W, Chen I H, Gludovatz B, Zimmermann E A, Ritchie R O and Meyers M A 2013 Natural flexible dermal armor *Adv. Mater.* **25** 31–48
- [9] Colorado State University 2012 *Warren and Genevieve Grast Photographic Collection, Archives and Special Collections* (Colorado State University)
- [10] In water Research Group Inc. 2013 (Jensen Beach, FL)
- [11] Barthelat F 2010 Nacre from mollusk shells: a model for high-performance structural materials *Bioinspir. Biomim.* **5** 035001
- [12] Roeder B A, Kokini K, Sturgis J E, Robinson J P and Voytki-Harbin S L 2002 Tensile mechanical properties of three-dimensional type I collagen extracellular matrices with varied microstructure *J. Biomech. Eng.* **124** 214
- [13] Broos J P F and Gunters R 2007 Study on the ballistic performance of monolithic ceramic plates *23rd Int. Symp. on Ballistics (Tarragona, Spain)* pp 1561–7
- [14] Larsen II J A and Cross C W 2007 Composite segmented flexible armor *US Patent Specification 2007/0234458 A1*

- [15] Patel P J, Hsieh A J and Gilde G A 2006 Improved low-cost multi-hit transparent armor *Army Research Report* ADA481074 (Adelphi, MD: US Army Research Laboratory)
- [16] Neal M L and Bain A D 2001 Method and apparatus for defeating high-velocity projectiles *US Patent Specification* 6170378 B1
- [17] Huang J, Durden H and Chowdhury M 2011 Bio-inspired armor protective material systems for ballistic shock mitigation *Mater. Design* **32** 3702–10
- [18] Ashby M 2013 Designing architected materials *Scr. Mater.* **68** 4–7
- [19] Barthelat F and Zhu D 2011 A novel biomimetic material duplicating the structure and mechanics of natural nacre *J. Mater. Res.* **26** 1203–15
- [20] Browning A, Ortiz C and Boyce M C 2013 Mechanics of composite elasmoid fish scale assemblies and their bioinspired analogues *J. Mech. Behav. Biomed. Mater.* **19** 75–86
- [21] Chai H and Lawn B R 2004 Fracture mode transitions in brittle coatings on compliant substrates as a function of thickness *J. Mater. Res.* **19** 1752–61
- [22] Chai H 2009 Indentation-induced subsurface tunneling cracks as a means for evaluating fracture toughness of brittle coatings *Int. J. Fract.* **158** 15–26
- [23] ANSYS Inc. 2013 ANSYSv13.0 (Canonsburg PA, USA)
- [24] Miranda P, Pajares A, Guiberteau F, Deng Y and Lawn B R 2003 Designing damage-resistant brittle-coating structures: I. Bilayers *Acta Mater.* **51** 4347–56